JACS
JOURNAL OF THE AMERICAN CHEMICAL SOCIETY

Communication

pubs.acs.org/JACS

Homochiral [2]Catenane and Bis[2]catenane from Alleno-Acetylenic Helicates - A Highly Selective Narcissistic Self-Sorting Process

Ori Gidron, Michael Jirásek, Nils Trapp, Marc-Olivier Ebert, Xiangyang Zhang, and François Diederich*

Laboratory of Organic Chemistry, ETH Zurich, Vladimir-Prelog-Weg 3, CH-8093 Zurich, Switzerland

Supporting Information

ABSTRACT: Homochiral strands of alternating alleno-acetylenes and phenanthroline ligands (*P*)-**1** and (P_2)-**2**, as well as their corresponding enantiomers, selectively assemble with the addition of silver(I) salt to yield dinuclear and trinuclear double helicates, respectively. Upon increasing the solvent polarity, the dinuclear and trinuclear helicates interlock to form a [2]catenane and bis[2]catenane, bearing 14 chirality elements, respectively. The solid-state structure of the [2]catenane reveals a nearly perfect fit of the interlocked strands, and the ECD spectra show a significant amplification of the chiroptical properties upon catenation, indicating stabilization of the helical secondary structure. Highly selective narcissistic self-sorting was demonstrated for a racemic mixture consisting of both short and long alleno-acetylenic strands, highlighting their potential for the preparation of linear catenanes of higher order.

Mechanically interlocked molecules, catenanes, besides rotaxanes and knots, have been fascinating chemists for the past decades, owing to their structural beauty as well as for their potential applications as molecular switches, selective hosts, and even as 2D chainmail networks.[1,2] Catenation is also observed in biomolecules such as DNA and proteins.[3] The most common structural feature is the simple Hopf link,[4] with only a handful of higher-order links reported, such as the Solomon link,[5] Borromean rings,[6] and the star of David.[7,8] Only few examples of homochiral catenanes have been reported.[9] To date, there is no general method to cleanly produce catenanes of higher complexity or to control their stereochemistry.[1d] While [*n*]catenanes can be assembled from *n* macrocycles as demonstrated by Sauvage,[10] Stoddart,[11] Stang,[12] Sanders,[13] and others,[14] this process often yields a mixture of catenanes in various sizes.

In this respect, self-sorting processes are crucial for the formation of large supramolecular assemblies in a multi-component environment.[15,16] Social self-sorting is relatively common and was previously demonstrated by Fujita for a dynamic catenation process,[17] but narcissistic self-sorting is far less abundant.[15] While narcissistic chiral self-sorting was demonstrated for metallacycles formed from chiral ligands,[18] no such example is known for catenanes.[19] Composed of several mechanically interlocked macrocycles, catenanes represent structures of higher complexity and are therefore more prone to yield undesired assemblies. Side products in the form of "meso" catenanes should be considered as well as cross-catenation (interlocking of different macrocycles).[17] Indeed, the catenation of a racemic mixture of (*R*)- and (*S*)-binaphthyl ligands led to "meso" (*RS*) rather than enantiopure (*RR* and *SS*) catenanes.[20] Spontaneous resolution was observed by Stoddart for [2]catenanes with planar chirality only upon crystallization, while the "meso" compound was always present in solution.[21]

Our group introduced enantiomerically pure 1,3-alleno-acetylenes as stable building blocks for the construction of optically active macrocycles and acyclic oligomers featuring all-carbon backbones and outstanding chiroptical properties.[22] We used these building blocks to construct enantiopure triple-stranded helicates from ligands (*P*)-**1** and (*M*)-**1**, with a helical cage ("helicage") for the encapsulation and detection of small organic molecules.[23] The formation of this cavity resulted from a combination of the lean alleno-acetylenic moieties and the all-carbon backbone. We were therefore interested in exploring further topologies formed by these scaffolds.

Here, we report the highly selective catenation of the homochiral alleno-acetylenic strands (*P*)-**1** and (P_2)-**2** (Scheme 1) and their corresponding enantiomers.[24] The strands assemble with silver(I) to form helicates (Δ_2)-(P_2)-**3** and (Δ_3)-(P_4)-**4**, which reversibly catenate to form [2]catenane (Δ_4)-(P_4)-**5** and bis[2]catenane (Δ_6)-(P_8)-**6**, respectively. A significant enhancement of chiroptical properties was observed for both catenanes with respect to the corresponding helicates. When a racemic mixture containing (*M*/*P*)-**1** and (M_2/P_2)-**2** was mixed with silver(I), a clean conversion either to helicates (Λ_2M_2/Δ_2P_2)-**3**

Scheme 1. Structures of Ligands, Helicates, and Catenanes

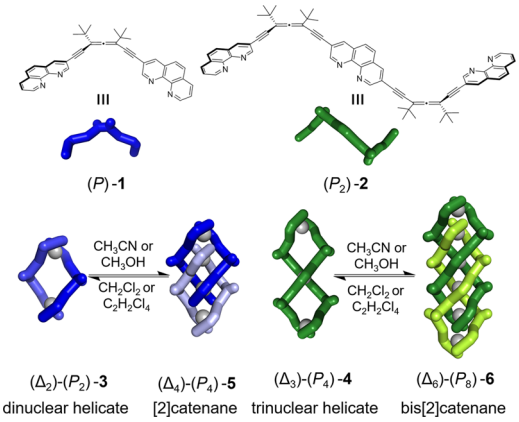

Received: August 15, 2015
Published: September 18, 2015

DOI: 10.1021/jacs.5b08649
J. Am. Chem. Soc. 2015, 137, 12502−12505

and $(\Lambda_3M_4/\Delta_3P_4)$-**4** or to catenanes $(\Lambda_4M_4/\Delta_4P_4)$-**5** and $(\Lambda_6M_8/\Delta_6P_8)$-**6** was observed with no cross-catenation or formation of "meso" catenanes, demonstrating a high degree of narcissistic self-sorting.

Mixing solutions of (*P*)-**1** with $AgPF_6$ or AgOTf in CD_2Cl_2 in a ratio of 1:1 resulted in the clean formation of double stranded helicate (Δ_2)-(P_2)-**3**. The ^{1}H NMR spectrum (Figure 1a) displayed only 7 aromatic signals (a–g) corresponding to the formation of a single species and excluding the formation of nonsymmetrical "mesocate" (nonhelical conformer with the two metal centers in the Δ,Λ conformation). Rotating frame nuclear Overhauser effect spectroscopy (ROESY) NMR reveals correlation between H^h located on the *tert*-butyl (^{t}Bu) and H^f (Figure S27, see SI), confirming that the phenanthroline (phen) conformation is the same as observed for the free ligand. This should result in right-handed helicates for (*P*)-**1** and left-handed helicates for (*M*)-**1** ligands. Upon switching to more polar solvents (CD_3OD or CD_3CN), the symmetry breaks, and a new set of 14 peaks appears, which can be assigned to the 14 aromatic protons (a–g and a′–g′, Figure 1b) of the inner and outer phen in an interlocked structure. Particularly noticeable is the upfield shift of $H^{b'}$ to 6.39 ppm, whereas the analogous H^b is shifted downfield to 8.09 ppm ($\Delta\delta$ = 1.70 ppm), indicating significantly different chemical environments. Such upfield shift for $H^{b'}$ is expected when the two phen moieties adopt a parallel-displaced alignment relative to each other, resulting in significant shielding of $H^{b'}$ by the π system of the outer phen and deshielding of the external H^b.[25] Indeed, ROESY NMR reveals correlation between the inner and outer phens and with $H^{a'}$ and H^g protons in close proximity (Figure 1c) as well as a correlation between $H^{b'}$ and H^h located on the ^{t}Bu moiety (Figure 1d), both consistent with the formation of [2]catenane (Δ_4)-(P_4)-**5** (Figure 1).

While [2]catenane (Δ_4)-(P_4)-**5** represents a common structural motif (Hopf link), we were interested in exploring new morphologies by extending the chiral strands. We therefore synthesized ligands (P_2)-**2** and (M_2)-**2** consisting of two allenoacetylenic and three phen units (see the SI for synthetic details). Mixing (P_2)-**2** with $AgPF_6$ or AgOTf in a ratio of 2:3 in $(CDCl_2)_2$ resulted in the formation of double helicate (Δ_3)-(P_4)-**4**, as indicated by 10 phen resonances in the ^{1}H NMR spectrum expected for a C_2 symmetric helicate (Figure 2a).[26] In addition,

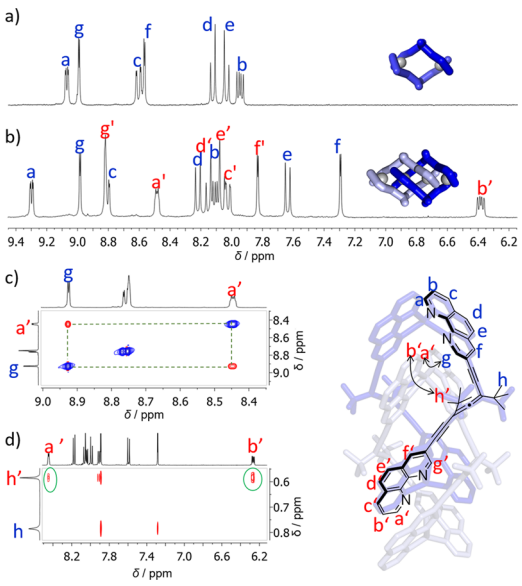

Figure 1. ^{1}H NMR spectra of (a) (Δ_2)-(P_2)-**3** in CD_2Cl_2 and (b) (Δ_4)-(P_4)-**5** in CD_3CN measured at 298 K. (c) and (d) Expansion of the ROESY NMR spectrum of (Δ_4)-(P_4)**5** in CD_3CN measured at 253 K.

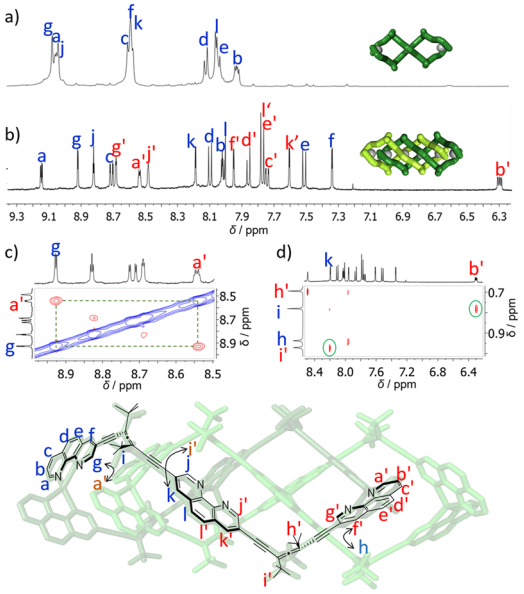

Figure 2. ^{1}H NMR spectra of (a) (Δ_3)-(P_4)-**4** in $(CDCl_2)_2$ and (b) (Δ_6)-(P_8)-**6** in CD_3CN at 298 K. (c) and (d) Expansion of the ROESY NMR spectrum of (Δ_6)-(P_8)-**6** in CD_3CN measured at 298 K.

ROESY correlation is observed between the ^{t}Bu protons and both H^k and H^f as expected for the helicate conformations (Figure S34 in SI). Upon dissolving in CD_3CN, the symmetry breaks, resulting in a total of 20 phen signals, displaying similar features to those observed for (Δ_4)-(P_4)-**5**. The resonance of $H^{b'}$ is shifted upfield ($\Delta\delta$ = 1.70 ppm) relative to H^b (Figure 2b). The ROESY NMR spectrum reveals correlation between $H^{a'}$ and H^g, between $H^{b'}$ and H^i, and between H^k and $H^{i'}$ (Figure 2c,d, respectively). Overall, the NMR spectra provide strong evidence that (Δ_6)-(P_8)-**6** is interlocked in a similar manner to (Δ_4)-(P_4)-**5**, yielding a bis[2]catenane structure. The reversibility of catenane/helicate transformation was tested for both catenanes by redissolving the catenanes in CD_2Cl_2 or $(CDCl_2)_2$, which resulted in complete reversion to the helicates (see SI Section S5).

At room temperature (RT), cross peaks could be observed by ROESY NMR between the two sets of peaks of (Δ_4)-(P_4)-**5**, an indication of dynamic exchange on the NMR time scale. This allowed to study the kinetics of the dynamic catenation process by varying the mixing times at different temperatures (see SI).[27] The values of $\Delta H^{\ddagger}$ = 12.4 kcal mol^{-1} and $\Delta G^{\ddagger}$ = 17.4 kcal mol^{-1} are in agreement with the observation that catenation readily takes place at RT. The negative value of $\Delta S^{\ddagger}$ = −16.9 cal K^{-1} mol^{-1} is an indication of an associative transition state. In contrast, no cross-correlation could be observed between the inner and outer protons for (Δ_6)-(P_8)-**6**, even upon heating to 65 °C, an indication that the dynamic catenation process is slow on the NMR time scale for the longer bis[2]catenane. The third metal coordination most likely reduces the rate of ligand dissociation.

The ESI-MS analysis of (Δ_2)-(P_2)-**3** and (Δ_3)-(P_4)-**4** reveals the influence of the solvent polarity on the catenane↔helicate equilibrium. In CH_2Cl_2, helicate $[(\Delta_2)$-(P_2)-**3**$]^{2+}$ is exclusively dominating, while in CH_3CN, the [2]catenane $[(\Delta_4)$-(P_4)-**5**$]^{4+}$ is

DOI: 10.1021/jacs.5b08649
J. Am. Chem. Soc. 2015, 137, 12502−12505

clearly detectable (~30%) and co-existent with the helicate $[(\Delta_2)\text{-}(P_2)\text{-}\mathbf{3}]^{2+}$. In a similar but more pronounced manner, the ESI-MS of $(\Delta_3)\text{-}(P_4)$-**4** in CH_2Cl_2 showed the expected $[(\Delta_3)\text{-}(P_4)\text{-}\mathbf{4}]^{3+}$ species with a small ratio of $[(\Delta_6)\text{-}(P_8)\text{-}\mathbf{6}]^{6+}$, while in CH_3CN the ions of bis[2]catenane $(\Delta_6)\text{-}(P_8)$-**6** are prevailingly observed (see SI Section S3.8).

The X-ray structure of single crystals of $(\Delta_4)\text{-}(P_4)$-**5** obtained by slow evaporation of methanol confirms the expected interlocked motif (Figure 3). The distance between $H^{b'}$ and

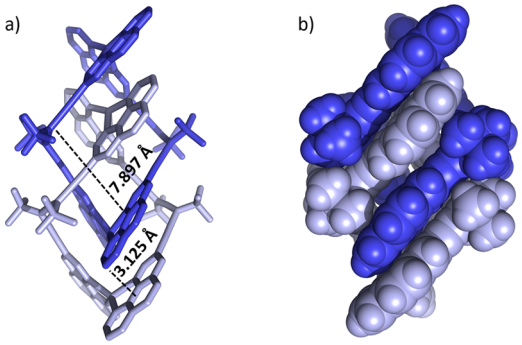

Figure 3. X-ray crystal structure of $(\Delta_4)\text{-}(P_4)$-**5** in (a) stick and (b) space filling representations. Counter anions, solvent molecules, and hydrogens (in (a)) were omitted for clarity.

the plane of the outer phen is 3.125 Å. Such proximity can explain the significant chemical shift of the inner and outer sets of protons, as observed in the ^{1}H NMR spectrum. In addition, the short distance of 2.206 Å between H^g and $H^{a'}$ is consistent with the strong ROESY correlation observed between these protons. The parallel-displaced alignment of the phen units supports the assumption that the driving forces for catenation in the more polar media are enthalpically favored cavity desolvation and $\pi-\pi$ interactions,[28] overcoming the entropically favored helicate formation.[29] The average distance between the two acetylenic carbons and the parallel phen plane is 7.897 Å, providing suitable space for intercalation. Indeed, the space-filling model shows a nearly perfect fit of the interlocked helicate (Figure 3b).

The intensity of the ECD spectra was found to be significantly stronger for catenanes than for the corresponding helicates. For example, the $\Delta\varepsilon$ values for $(\Delta_6)\text{-}(P_8)$-**6** are by up to 2.5-fold higher, compared with $(\Delta_3)\text{-}(P_4)$-**4** (measured with the same ligand molarity).[9a] This amplification presumably results from rigidification of the secondary helical structure, with the interlocked assemblies reducing the conformational "wiggling" compared with the corresponding helicate (see Section S6 in the SI for detailed analysis).

We have previously reported the enantioselective self-sorting of triple helicates consisting of racemic (M/P)-**1**.[23] It was therefore not surprising that self-sorting was also observed for the assembly in the presence of silver(I) ions of both helicates $(\Lambda_2M_2/\Delta_2P_2)$-**3** and $(\Lambda_3M_4/\Delta_3P_4)$-**4** from racemic mixtures of (M/P)-**1** or (M_2/P_2)-**2**, respectively. While narcissistic self-sorting of helicates is commonly observed, and is in fact rather the rule than the exception,[30] this is not the case for catenanes. Narcissistic self-sorting is more challenging in such systems, since catenation can also result from the interaction of Δ and Λ helicates. To ultimately test the sorting of a 4-component system, we combined racemic mixtures $(\Lambda_2M_2/\Delta_2P_2)$-**3** and $(\Lambda_3M_4/\Delta_3P_4)$-**4**, redissolved in acetonitrile (Figure 4). Complete enantioselective and stereoselective narcissistic self-sorting was observed for both the helicates and the catenanes. The ^{1}H NMR

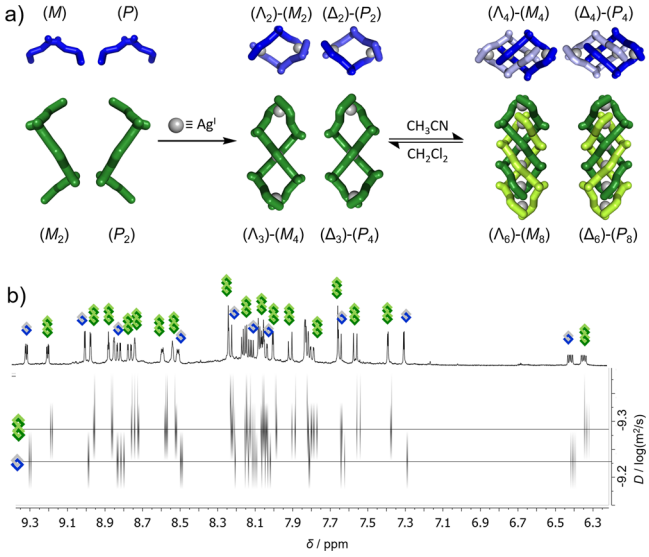

Figure 4. (a) Narcissistic self-sorting in a racemic mixture of (M/P)-**1** and (M_2/P_2)-**2** to yield $(\Lambda_2M_2/\Delta_2P_2)$-**3** and $(\Lambda_3M_4/\Delta_3P_4)$-**4** or $(\Lambda_4M_4/\Delta_4P_4)$-**5** and $(\Lambda_6M_8/\Delta_6P_8)$-**6**. (b) ^{1}H and DOSY NMR spectrum of a mixture containing racemic $(\Lambda_4M_4/\Delta_4P_4)$-**5** and $(\Lambda_6M_8/\Delta_6P_8)$-**6** in CD_3CN, measured at 298 K. Blue rhombus represents $(\Lambda_4M_4/\Delta_4P_4)$-**5** and green rhombus represents $(\Lambda_6M_8/\Delta_6P_8)$-**6**.

spectrum shows only two sets of peaks corresponding to $(\Lambda_4M_4/\Delta_4P_4)$-**5** and $(\Lambda_6M_8/\Delta_6P_8)$-**6**, and the DOSY NMR spectrum clearly shows the two different catenanes, with the smaller $(\Lambda_4M_4/\Delta_4P_4)$-**5** displaying a faster diffusion rate than $(\Lambda_6M_8/\Delta_6P_8)$-**6** (Figure 4b). Importantly, no "meso" catenanes, previously observed for similar systems,[20] or of any mixed species consisting of short and long helicates were detected. We explain the high degree of self-sorting in our system by the combination of relatively rigid ligand systems, with no sp^3 carbons in the backbone as well as by the nearly perfect fit of the interlocked structures.

In conclusion, we demonstrated the selective metal ion-mediated assembly of short and long alleno-acetylenic ligands to double-stranded helicates, which reversibly form [2]catenane and bis[2]catenanes, respectively. The X-ray structure of the [2]catenane reveals a perfect fit for the interlocked strands, and ECD spectra demonstrate significantly stronger Cotton effect for the catenanes over the corresponding helicates, indicating a more rigid structure. Highly selective narcissistic self-sorting is demonstrated for a racemic mixture, consisting of both short and long ligands. It is reasonable to assume that further elongation of the alleno-acetylenic strands can result in even longer catenanes, and we therefore suggest this method for the selective assembly of poly[2]catenanes from *n* nuclear helicates.

■ ASSOCIATED CONTENT

Supporting Information

The Supporting Information is available free of charge on the ACS Publications website at DOI: 10.1021/jacs.5b08649.

Synthesis and full characterization of new compounds, X-ray crystallographic data, details of kinetic measurements (PDF)

Crystallographic data (CIF)

DOI: 10.1021/jacs.5b08649
J. Am. Chem. Soc. 2015, 137, 12502−12505

AUTHOR INFORMATION

Corresponding Author

*diederich@org.chem.ethz.ch

Notes

The authors declare no competing financial interest.

ACKNOWLEDGMENTS

This work was funded by the Swiss National Science Foundation. O.G. acknowledges a Marie-Curie fellowship (no. 327582) from the EU FP7 program, and M.J. a Swiss-European Mobility Grant. We are grateful to Michael Solar from the Small Molecule Crystallography Center at ETH Zurich (http://www.smocc.ethz.ch), Dr. Bruno Bernet, Dr. David Schweinfurth, and Jovana Millic for comments and suggestions, and Prof. Reiner Herges for his help with the topological analysis.

REFERENCES

(1) (a) *Molecular Catenanes, Rotaxanes and Knots: A Journey Through the World of Molecular Topology*Sauvage, J.-P., Dietrich-Buchecker, C., Eds.; Wiley-VCH: Weinheim, Germany, 1999. (b) Fang, L.; Olson, M. A.; Benítez, D.; Tkatchouk, E.; Goddard, W. A.; Stoddart, J. F. *Chem. Soc. Rev.* **2010**, *39*, 17−29. (c) Evans, N. H.; Beer, P. D. *Chem. Soc. Rev.* **2014**, *43*, 4658−4683. (d) Gil-Ramírez, G.; Leigh, D. A.; Stephens, A. J. *Angew. Chem., Int. Ed.* **2015**, *54*, 6110−6150. (e) Cook, T. R.; Stang, P. J. *Chem. Rev.* **2015**, *115*, 7001−7045.

(2) (a) Yamashita, K.-i.; Kawano, M.; Fujita, M. *J. Am. Chem. Soc.* **2007**, *129*, 1850−1851. (b) Lee, H.; Elumalai, P.; Singh, N.; Kim, H.; Lee, S. U.; Chi, K.-W. *J. Am. Chem. Soc.* **2015**, *137*, 4674−4677. (c) Thorp-Greenwood, F. L.; Kulak, A. N.; Hardie, M. J. *Nat. Chem.* **2015**, *7*, 526−531.

(3) (a) Clayton, D. A.; Vinograd, J. *Nature* **1967**, *216*, 652−657. (b) Wikoff, W. R.; Liljas, L.; Duda, R. L.; Tsuruta, H.; Hendrix, R. W.; Johnson, J. E. *Science* **2000**, *289*, 2129−2133.

(4) (a) Dietrich-Buchecker, C. O.; Sauvage, J. P.; Kern, J. M. *J. Am. Chem. Soc.* **1984**, *106*, 3043−3045. (b) Vögtle, F.; Meier, S.; Hoss, R. *Angew. Chem., Int. Ed. Engl.* **1992**, *31*, 1619−1622. (c) Nierengarten, J. F.; Dietrich-Buchecker, C. O.; Sauvage, J.-P. *J. Am. Chem. Soc.* **1994**, *116*, 375−376. (d) Mohr, B.; Sauvage, J.-P.; Grubbs, R. H.; Weck, M. *Angew. Chem., Int. Ed. Engl.* **1997**, *36*, 1308−1310. (e) Dietrich-Buchecker, C.; Sauvage, J.-P. *Chem. Commun.* **1999**, *7*, 615−616. (f) Hovorka, R.; Meyer-Eppler, G.; Piehler, T.; Hytteballe, S.; Engeser, M.; Topić, F.; Rissanen, K.; Lützen, A. *Chem. - Eur. J.* **2014**, *20*, 13253−13258. (g) Robinson, S. W.; Mustoe, C. L.; White, N. G.; Brown, A.; Thompson, A. L.; Kennepohl, P.; Beer, P. D. *J. Am. Chem. Soc.* **2015**, *137*, 499−507.

(5) Pentecost, C. D.; Chichak, K. S.; Peters, A. J.; Cave, G. W. V.; Cantrill, S. J.; Stoddart, J. F. *Angew. Chem., Int. Ed.* **2007**, *46*, 218−222.

(6) Chichak, K. S.; Cantrill, S. J.; Pease, A. R.; Chiu, S.-H.; Cave, G. W. V.; Atwood, J. L.; Stoddart, J. F. *Science* **2004**, *304*, 1308−1311.

(7) Leigh, D. A.; Pritchard, R. G.; Stephens, A. J. *Nat. Chem.* **2014**, *6*, 978−982.

(8) For other higher-order structures, see: (a) Wood, C. S.; Ronson, T. K.; Belenguer, A. M.; Holstein, J. J.; Nitschke, J. R. *Nat. Chem.* **2015**, *7*, 354−358. (b) Wang, Q.; Yu, C.; Long, H.; Du, Y.; Jin, Y.; Zhang, W. *Angew. Chem., Int. Ed.* **2015**, *54*, 7550−7554.

(9) (a) Hori, A.; Akasaka, A.; Biradha, K.; Sakamoto, S.; Yamaguchi, K.; Fujita, M. *Angew. Chem., Int. Ed.* **2002**, *41*, 3269−3272. (b) Theil, A.; Mauve, C.; Adeline, M. T.; Marinetti, A.; Sauvage, J.-P. *Angew. Chem., Int. Ed.* **2006**, *45*, 2104−2107. (c) Penticost, C. D.; Peters, A. J.; Chichak, K. S.; Cave, G. W. V.; Cantrill, S. J.; Stoddart, J. F. *Angew. Chem., Int. Ed.* **2006**, *45*, 4099−4104. (d) Nakatani, Y.; Furusho, Y.; Yashima, E. *Angew. Chem., Int. Ed.* **2010**, *49*, 5463−5467. (e) Zhang, G.; Gil-Ramirez, G.; Markevicius, A.; Browne, C.; Vitorica-Yrezabal, I. J.; Leigh, D. A. *J. Am. Chem. Soc.* **2015**, *137*, 10437−10442.

(10) Bitsch, F.; Dietrich-Buchecker, C. O.; Khémiss, A.-K.; Sauvage, J.-P.; Van Dorsselaer, A. *J. Am. Chem. Soc.* **1991**, *113*, 4023−4025.

(11) Amabilino, D. B.; Ashton, P. R.; Reder, A. S.; Spencer, N.; Stoddart, J. F. *Angew. Chem., Int. Ed. Engl.* **1994**, *33*, 1286−1290.

(12) Li, S.; Huang, J.; Cook, T. R.; Pollock, J. B.; Kim, H.; Chi, K.-W.; Stang, P. J. *J. Am. Chem. Soc.* **2013**, *135*, 2084−2087.

(13) Cougnon, F. B. L.; Jenkins, N. A.; Pantoş, G. D.; Sanders, J. K. M. *Angew. Chem., Int. Ed.* **2012**, *51*, 1443−1447.

(14) (a) Hori, A.; Kumazawa, K.; Kusukawa, T.; Chand, D. K.; Fujita, M.; Sakamoto, S.; Yamaguchi, K. *Chem. - Eur. J.* **2001**, *7*, 4142−4149. (b) Wang, L.; Vysotsky, M. O.; Bogdan, A.; Bolte, M.; Böhmer, V. *Science* **2004**, *304*, 1312−1314. (c) Langton, M. J.; Matichak, J. D.; Thompson, A. L.; Anderson, H. L. *Chem. Sci.* **2011**, *2*, 1897−1901. (d) Black, S. P.; Stefankiewicz, A. R.; Smulders, M. M. J.; Sattler, D.; Schalley, C. A.; Nitschke, J. R.; Sanders, J. K. M. *Angew. Chem., Int. Ed.* **2013**, *52*, 5749−5752.

(15) Wu, A.; Isaacs, L. *J. Am. Chem. Soc.* **2003**, *125*, 4831−4835.

(16) (a) Johnson, A. M.; Wiley, C. A.; Young, M. C.; Zhang, X.; Lyon, Y.; Julian, R. R.; Hooley, R. J. *Angew. Chem., Int. Ed.* **2015**, *54*, 5641−5645. (b) Makiguchi, W.; Tanabe, J.; Yamada, H.; Iida, H.; Taura, D.; Ousaka, N.; Yashima, E. *Nat. Commun.* **2015**, *6*, 7236.

(17) Hori, A.; Yamashita, K.-I.; Fujita, M. *Angew. Chem., Int. Ed.* **2004**, *43*, 5016−5019.

(18) Gütz, C.; Hovorka, R.; Schnakenburg, G.; Lützen, A. *Chem. - Eur. J.* **2013**, *19*, 10890−10894.

(19) The self-sorting behavior of molecular knots was recently reported: Ayme, J.-F.; Beves, J. E.; Campbell, C. J.; Leigh, D. A. *Angew. Chem., Int. Ed.* **2014**, *53*, 7823−7827.

(20) Burchell, T. J.; Eisler, D. J.; Puddephatt, R. J. *Dalton Trans.* **2005**, 268−272.

(21) Ashton, P. R.; Boyd, S. E.; Menzer, S.; Pasini, D.; Raymo, F. M.; Spencer, N.; Stoddart, J. F.; White, A. J. P.; Williams, D. J.; Wyatt, P. G. *Chem. - Eur. J.* **1998**, *4*, 299−310.

(22) (a) Alonso-Gómez, J. L.; Rivera-Fuentes, P.; Harada, N.; Berova, N.; Diederich, F. *Angew. Chem., Int. Ed.* **2009**, *48*, 5545−5548. (b) Rivera-Fuentes, P.; Alonso-Gómez, J. L.; Petrovic, A. G.; Santoro, F.; Harada, N.; Berova, N.; Diederich, F. *Angew. Chem., Int. Ed.* **2010**, *49*, 2247−2250. (c) Donckele, E. J.; Gidron, O.; Trapp, N.; Diederich, F. *Chem. - Eur. J.* **2014**, *20*, 9558−9566.

(23) Gidron, O.; Ebert, M.-O.; Trapp, N.; Diederich, F. *Angew. Chem., Int. Ed.* **2014**, *53*, 13614−13618.

(24) For simplicity, the preparation and characterization of one enantiomer will mostly be discussed throughout the text. We note, however, that for all presented structures and assemblies, both enantiomers were synthesized and characterized.

(25) Poudel, P. P.; Chen, J.; Cammers, A. *Eur. J. Org. Chem.* **2008**, *2008*, 5511−5517.

(26) Gütz, C.; Hovorka, R.; Struch, N.; Bunzen, J.; Meyer-Eppler, G.; Qu, Z.-W.; Grimme, S.; Topić, F.; Rissanen, K.; Cetina, M.; Engeser, M.; Lützen, A. *J. Am. Chem. Soc.* **2014**, *136*, 11830−11838.

(27) Fujita, M.; Ibukuro, F.; Seki, H.; Kamo, O.; Imanari, M.; Ogura, K. *J. Am. Chem. Soc.* **1996**, *118*, 899−900.

(28) (a) Meyer, E. A.; Castellano, R. K.; Diederich, F. *Angew. Chem., Int. Ed.* **2003**, *42*, 1210−1250. (b) Barin, G.; Coskun, A.; Fouda, M. M. G.; Stoddart, J. F. *ChemPlusChem* **2012**, *77*, 159−185. (c) Biedermann, F.; Nau, W. M.; Schneider, H.-J. *Angew. Chem., Int. Ed.* **2014**, *53*, 11158−11171. (d) Persch, E.; Dumele, O.; Diederich, F. *Angew. Chem., Int. Ed.* **2015**, *54*, 3290−3327.

(29) (a) Fujita, M.; Ibukuro, F.; Yamaguchi, K.; Ogura, K. *J. Am. Chem. Soc.* **1995**, *117*, 4175−4176. (b) Fujita, M. *Acc. Chem. Res.* **1999**, *32*, 53−61.

(30) Krämer, R.; Lehn, J.-M.; Marquis-Rigault, A. *Proc. Natl. Acad. Sci. U. S. A.* **1993**, *90*, 5394−5398.

DOI: 10.1021/jacs.5b08649
J. Am. Chem. Soc. 2015, 137, 12502−12505